# Radiation Induced Redox Reactions and Fragmentation of Constituent Ions in Ionic Liquids. 2. Imidazolium Cations

**ARTICLE** *in* THE JOURNAL OF PHYSICAL CHEMISTRY B · MARCH 2011

Impact Factor: 3.3 · DOI: 10.1021/jp200305b · Source: PubMed



**5 AUTHORS**, INCLUDING:

Ilya Shkrob
Argonne National Laboratory
**143** PUBLICATIONS **2,164** CITATIONS
SEE PROFILE

Timothy W Marin
Benedictine University
**54** PUBLICATIONS **810** CITATIONS
SEE PROFILE

Sergey D Chemerisov
Argonne National Laboratory
**80** PUBLICATIONS **929** CITATIONS
SEE PROFILE

James Wishart
Brookhaven National Laboratory
**115** PUBLICATIONS **3,642** CITATIONS
SEE PROFILE

THE JOURNAL OF PHYSICAL CHEMISTRY B

ARTICLE

pubs.acs.org/JPCB

# Radiation Induced Redox Reactions and Fragmentation of Constituent Ions in Ionic Liquids. 2. Imidazolium Cations

Ilya A. Shkrob,*[,†] Timothy W. Marin,[†,‡] Sergey D. Chemerisov,[†] Jasmine L. Hatcher,[§] and James F. Wishart[§]

[†]Chemical Sciences and Engineering Division, Argonne National Laboratory, 9700 S. Cass Ave, Argonne, Illinois 60439, United States

[‡]Chemistry Department, Benedictine University, 5700 College Road, Lisle, Illinois 60532, United States

[§]Chemistry Department, Brookhaven National Laboratory, Upton, New York 11973-5000, United States

Supporting Information

**ABSTRACT:** In part 1 of this study, radiolytic degradation of constituent anions in ionic liquids (ILs) was examined. The present study continues the themes addressed in part 1 and examines the radiation chemistry of 1,3-dialkyl substituted imidazolium cations, which currently comprise the most practically important and versatile class of ionic liquid cations. For comparison, we also examined 1,3-dimethoxy- and 2-methyl-substituted imidazolium and 1-butyl-4-methylpyridinium cations. In addition to identification of radicals using electron paramagnetic resonance spectroscopy (EPR) and selective deuterium substitution, we analyzed stable radiolytic products using $^{1}H$ and $^{13}C$ nuclear magnetic resonance (NMR) and tandem electrospray ionization mass spectrometry (ESMS). Our EPR studies reveal rich chemistry initiated through "ionization of the ions": oxidation and the formation of radical dications in the aliphatic arms of the parent cations (leading to deprotonation and the formation of alkyl radicals in these arms) and reduction of the parent cation, yielding 2-imidazolyl radicals. The subsequent reactions of these radicals depend on the nature of the IL. If the cation is 2-substituted, the resulting 2-imidazolyl radical is relatively stable. If there is no substitution at C(2), the radical then either is protonated or reacts with the parent cation forming a C(2)−C(2) $\sigma\sigma^*$-bound dimer radical cation. In addition to these reactions, when methoxy or $C_\alpha$-substituted alkyl groups occupy the N(1,3) positions, their elimination is observed. The elimination of methyl groups from N(1,3) was not observed. Product analyses of imidazolium liquids irradiated in the very-high-dose regime (6.7 MGy) reveal several detrimental processes, including volatilization, acidification, and oligomerization. The latter yields a polymer with $m/z$ of 650 ± 300 whose radiolytic yield increases with dose (~0.23 monomer units per 100 eV for 1-methyl-3-butylimidazolium trifluorosulfonate). Gradual generation of this polymer accounts for the steady increase in the viscosity of the ILs upon irradiation. Previous studies at lower dose have missed this species due to its wide mass distribution (stretching out to $m/z$ 1600) and broad NMR lines, which make it harder to detect at lower concentrations. Among other observed changes is the formation of water immiscible fractions in hydrophilic ILs and water miscible fractions in hydrophobic ILs. The latter is due to anion fragmentation. The import of these observations for use of ILs as extraction solvents in nuclear cycle separations is discussed.

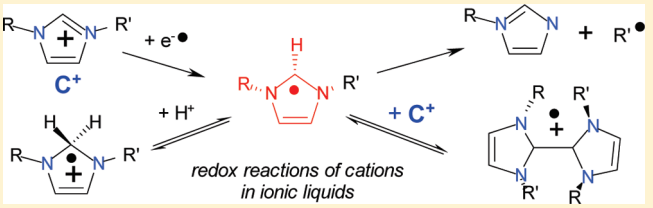


## 1. INTRODUCTION

The present study continues the themes addressed in part I of this two-part series:[1] radiolytically induced redox reactions and fragmentation of constituent ions in room-temperature ionic liquids (ILs). Currently, the largest class of practically important ionic liquids are those composed of 1,3- and 1,2,3-derivatized imidazolium cations (Scheme 1). In this study, we focus almost exclusively on such cations (some results for 1-butyl-4-methylpyridinium are given in section 3.3). The practical motivation for these studies is discussed in detail in part 1,[1] but generally it concerns their potential role in systems for recycling spent nuclear fuel. However, the observations made here could also apply to other uses of ionic liquids in extreme environments such as in spacecraft or lunar telescopes.[2,3]

The interaction of ionizing radiation with matter causes ionization and the formation of excited states (that are typically produced via the recombination of ionized molecules).[4−6] In molecular systems, this ionization generates *radical ions*. The same radical ions can be produced in electrochemical and photoinduced reactions.[6,7] In contrast, ionic liquids are *already* composed of ions. What kind of transient species are produced in their ionization and excitation?[6] Our study aims to answer this very basic question.

The "ionization of the ions" can be viewed either as electron detachment from the constituent anions ($A^-$) or the formation of radical dications from the constituent cations ($C^+$):

$$A^- \rightarrow A^\bullet + e^{-\bullet} \qquad (1)$$

**Received:** January 11, 2011
**Revised:** February 8, 2011
**Published:** March 18, 2011

**Scheme 1. Redox Chemistry of 1-Methyl-3-alkylimidazolium Cations in Ionic Liquids**[a]

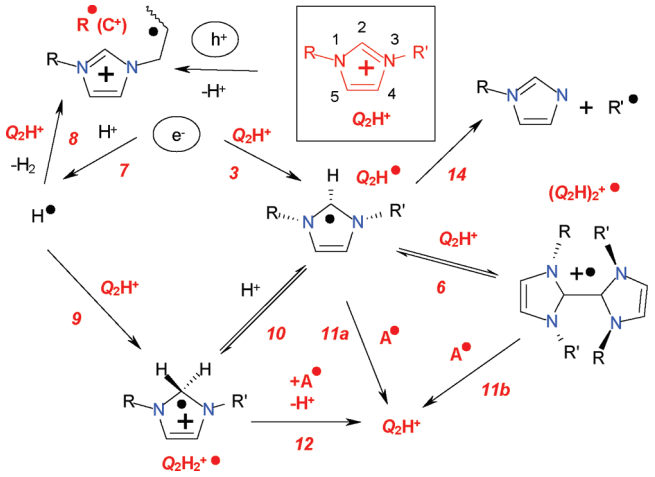


[a] The symbols and reaction numbering follow section 1.

$$C^{+} \rightarrow C^{2+\bullet} + e^{-\bullet} \quad (2)$$

The occurrence of reaction 2 is counterintuitive because the ionization potentials (IPs) of anions (i.e., the electron detachment energies) in a condensed-matter system can be low (3−5 eV)[1,4,8] and lowered still by electron attachment to the cation

$$C^{+} + e^{-\bullet} \rightarrow C^{\bullet} \quad (3)$$

On the other hand, removing an electron from the cation is an energetic process, although the energetic cost may be mitigated by interactions with neighboring anions. Either way, the energy expended in a typical ionization event in radiolysis is on the order of 5−10 eV, thus reaction 2 is possible.[4,6] Furthermore, some anions, such as $BF_4^-$ and $PF_6^-$, have high IPs whereas aliphatic cations (such as the alkyl derivatives of phosphonium, ammonium, piperidinium, pyrrolidinium, and morpholinium) have negative electron affinities (EAs) so that reaction 3 does not lower the barrier for charge separation. Another important factor is cation size. The constituent cations in ILs acquire their positive charge through the inclusion of group V (sometimes group VI) heteroatoms, so the positive charge is localized either on these heteroatoms or in the aromatic $\pi$-systems involving such heteroatoms. If the cation has long aliphatic arms, ionization in these arms is less hindered with regard to Coulomb repulsion, as the excess positive charge is sufficiently removed from the locus of the positive charge in the parent cation, whereas it lies close to the anions that surround the organic cation. While $C^{2+\bullet}$ might be fleetingly stabilized through such electrostatic interactions and polarization effects, such a species is unstable. As the excess charge in such radical dications tends to locate at the termini of their extended aliphatic arms,[4] this species either deprotonates, yielding the corresponding alkyl radical, $R^{\bullet}(C^{+})$, or accepts an electron from the nearest anion:

$$C^{2+\bullet} + A^{-} \rightarrow R^{\bullet}(C^{+}) + H^{+}A^{-} \quad (4)$$

$$C^{2+\bullet} + A^{-} \rightarrow C^{+} + A^{\bullet} \quad (5)$$

Our previous study[4] suggested that for aliphatic cations, reaction 4 is faster than reaction 5, as the yield of $R^{\bullet}(C^{+})$ is high and these alkyl radicals tend to be terminal and penultimate, which is consistent with deprotonation from the site of the maximum spin density. Such selectivity is typical for the deprotonation of alkane radical cations.[4] In contrast, for imidazolium cations, the yield of these radicals appeared to be low, and we took this observation as evidence for the relative stability of aromatic $C^{2+\bullet}$ due to the sharing of the excess charge by the imidazolium ring, which slows down deprotonation and facilitates reaction 5. This rationale is reconsidered in section 3.1: deprotonation of the cations is not unique to aliphatic ILs, as originally suggested. Since reaction 5 recovers the parent cation, it does not contribute to cation fragmentation, though it yields radical $A^{\bullet}$ that can readily undergo fragmentation, as discussed in part 1 of this series.[1]

Reactions 1 and 2 yield an excess electron. In aliphatic ILs, this electron may form a species resembling F-centers in ionic solids, in which the negative charge occupies an anion vacancy and electrostatically interacts with several nearby cations.[6,9,10] This light-absorbing electron species can be observed directly, using pulse radiolysis or laser excitation−transient absorption spectroscopy, as it strongly absorbs in the near-infrared and the visible.[9,10] At 300 K, this F-center can persist on a microsecond time scale.[9] In neat and relatively pure ILs, this species either decays by reaction with hole-derived species or by reaction with adventitious scavengers, including protic impurities (traces of acids) and certain halogenated anions, which react by dissociative electron attachment, releasing $F^-$.[1] The situation in aromatic ILs is less clear. One could expect that the imidazolium cation has a sufficiently high electron affinity with which to undergo reaction 3, yielding the corresponding 2-imidazolyl $\sigma$-radical (Scheme 1 and Table 2S in the Supporting Information). Such radicals are detected optically in pulse radiolysis of aqueous solutions of imidazolium salts[11,12] and exhibit strong absorption bands in the blue. These radical species are also detected, albeit indirectly, in muonium spin resonance, when a persistent imidazol-2-ylidenecarbene is bombarded by muons.[13] Spectroscopic evidence indicates that such radicals are also formed in the radiolysis of neat imidazolium liquids.[11,12] Our electron paramagnetic resonance (EPR) study of irradiated 1-methyl-3-alkylimidazolium ($C_n$mim$^+$) bistriflimide ($NTf_2^-$)[4] indicated the formation of a trapped-electron radical that we attributed to $C^{\bullet}$. This identification was tentative, as the spectrum was poorly resolved. Nevertheless, it was clear from these EPR results that even if the excess electron fleetingly exists in imidazolium ILs, this species would be short-lived, as the electron is eventually scavenged by the aromatic cations. We therefore suggested in ref 5 that the 2-imidazolyl radical undergoes 3-electron C−C $\sigma^1\sigma^{*2}$ bond formation with the parent cation forming a dimer radical cation,

$$C^{\bullet} + C^{+} \rightleftharpoons C_2^{+\bullet} \quad (6)$$

The low-energy $\sigma \leftarrow \sigma^*$ band of $C_2^{+\bullet}$ can easily be confused with the absorption band of the "solvated" electron. In fact, $C_2^{+\bullet}$ can be considered an extreme kind of such an electron.[5,7,14] In the gas phase, the dimer cation is bound by 0.5−1 eV, depending on the substitution in the 1,3-positions.[5] For 2-substituted imidazolium, reaction 6 is always endothermic. Since in the IL, the cation strongly interacts with several anions by Coulomb attraction, reaction 6 should be endothermic in ILs composed of small anions, as the Coulomb pairing energy is reduced for the $C_2^{+\bullet}$ cation (as it is larger than the parent cation). Thus, reaction 6 in the ILs is, in fact, reversible

and it can be shifted to either side. The initial electron trapping (in analogy to electron trapping in ionic solids) is likely to involve anion interstitials, and the absence of the counteranion near the trapping site can facilitate forward reaction 6, if only temporarily. Pulse radiolysis data for $C_n$mim $NTf_2$[5] indicated a transient absorption band in the visible and near-infrared that persisted for 10 ns in a room temperature solvent. This band was not from the monomer radical, suggesting the possibility of the formation of $C_2^{+\bullet}$ in this ionic liquid (see also the discussion in ref 14). Our moment analysis of the EPR spectrum of the cation-derived radical in frozen, irradiated $C_n$mim $NTf_2$ was consistent with this attribution.[5]

In this study, we examine EPR spectra of ionic liquids composed of imidazolium cations in more detail. Inter alia, we demonstrate that (i) reaction 3 always occurs in such ILs and (ii) in most of such ILs reaction 6 is shifted to the left side, whereas in some ILs (composed of large, fluorinated anions), this reaction is shifted to the right side. These observations resolve the existing inconsistencies concerning electron localization in imidazolium ILs.

However, it turns out that this chemistry is more complex than was realized by previous workers. In the following, we adapt the nomenclature in which the residue of the cation with respect to substitution in the *n*th atom in the ring (Scheme 1) is designated as $Q_n$. In this nomenclature, the parent cation is $Q_2H^+$, the 2-imidazolyl radical is $Q_2H^\bullet$, the carbene is $Q_2^{\bullet\bullet}$, etc. As protic impurities such as water are common in ILs and expected to be present in real-world applications, and protons are radiolytically generated in reaction 4, electron attachment reaction 3 competes with electron attachment to the proton (in the form of $H_3O^+$ or $H^+A^-$)

$$e^{-\bullet} + H^+ \rightarrow H^\bullet \tag{7}$$

yielding mobile, reactive hydrogen atoms. The latter can abstract hydrogen from aliphatic arms of the cation (Y = H, D) yielding $R^\bullet(C^+)$,

$$Y^\bullet + C^+ \rightarrow YH + R^\bullet(C^+) \tag{8}$$

and add to the 2-position of the imidazolium ring of the parent radical $Q_2X^+$, generating adduct radical cations $Q_2XY^{+\bullet}$,

$$Y^\bullet + Q_2X^+ \rightarrow Q_2XY^{+\bullet} \tag{9}$$

where X is a group substituting at C(2) in the parent cation. In part 1 of this series,[1] we demonstrated that in addition to atomic hydrogen, other small radicals ($R'^\bullet$), such as methyl and hydroxymethyl could react in a similar fashion, producing $Q_2XR'^{+\bullet}$. However, the same adduct radical that is generated via reaction 9 can also be produced by protonation of the $Q_2X^\bullet$ radical (or the dimer cation) generated in reaction 3,

$$H^+ + Q_2X^\bullet \rightleftharpoons Q_2XH^{+\bullet} \tag{10}$$

which may occur even if no hydrogen atoms are generated, provided that the proton affinity of $Q_2X^\bullet$ is sufficiently large to compete with the anion. It is well-known that carbenes $Q_2^{\bullet\bullet}$ are fairly strong bases that retain $H^+$ in ILs,[7,15] and calculations suggested that the proton affinity of $C^\bullet$ should be at least as high.[7] This suggests that in addition to back recombination,

$$C^\bullet + A^\bullet \rightarrow C^+ + A^- \tag{11a}$$

and the analogous reaction involving the dimer radical cation,

$$C_2^{+\bullet} + A^\bullet \rightarrow C^+ + C^+A^- \tag{11b}$$

the electron-trapped species $Q_2X^\bullet$ can undergo protonation followed by

$$Q_2XH^{+\bullet} + A^\bullet \rightarrow Q_2X^+ + H^+A^- \tag{12}$$

In section 3.1.4, we provide evidence that $Q_2XH^{+\bullet}$ radicals are generated in irradiated imidazolium ILs and can be produced either via reaction 9 or 10.

These reactions just described do not exhaust the richness of the radiation chemistry of imidazolium cations (Scheme 1). In the radiolysis of onium ILs, we were not able to produce EPR spectroscopic evidence for elimination of long aliphatic arms,[4] although such a process is hinted at by product analyses.[16−18] The loss of such arms may involve either cleavage at N(3) in the excited state of the cation

$$(Q_3R^+)^* \rightarrow Q_3H^+ + R(-H) \tag{13a}$$

with the formation of unsaturated species (such reactions were observed in $MS_2^+$ experiments for various imidazolium derivatives in the gas phase)[19] or homolytic dissociation of the parent cation

$$(Q_3R^+)^* \rightarrow Q_3^{+\bullet} + R^\bullet \tag{13b}$$

The similar reaction may also occur in the ground or excited states of the 2-imidazolyl radical:

$$Q_3R^\bullet \rightarrow Q_3 + R^\bullet \tag{14}$$

Reaction 13a is thought to be a C−N bond scission reaction 13b concerted with H transfer from the leaving group; deuteron substitution studies of Lesimple et al.[19] indicate that H-abstraction from $R^\bullet$ by $Q_3^{+\bullet}$ may occur from any position in the arm.

In section 3.1.2 we demonstrate that reaction 14 occurs in at least two IL systems, and in one of these systems it occurs in a delayed fashion as the sample is warmed, indicating that it indeed proceeds from the ground state of the 2-imidazolyl radical. We suggest that the lifetime of radiolytically generated 2-imidazolyl radicals in room-temperature ILs is reduced not only due to rapid radical recombination, reaction 11a, and association via reaction 6 but also due to the ease of protonation, reaction 10, and the loss of aliphatic arms, reaction 14.

For brevity, some EPR spectra and tables are placed in the Supporting Information. These have designator "S" (such as Figure 1S) and can be found in the Supporting Information.

## 2. EXPERIMENTAL METHODS

**2.1. Materials.** Experimental and computational approaches used in this study are the same as in part 1.[1] The identification of some imidazolium-derived radicals required selective deuteration in the imidazolium ring and in the arms. The deuteration in the ring followed the general method described in part 1 of this study[1] (see Table 1S, Supporting Information, for the isotope composition). The H/D substitution in the arms was carried out using the synthetic protocols described in section 1S of the Supporting Information. In the electron paramagnetic resonance (EPR) spectra (9.44 GHz) shown in section 3, the radiation-induced EPR signal from a silicon dangling bond center in the Suprasil sample tubes is removed. The samples used in EPR measurements were irradiated at 77 K to a total dose of 3 kGy

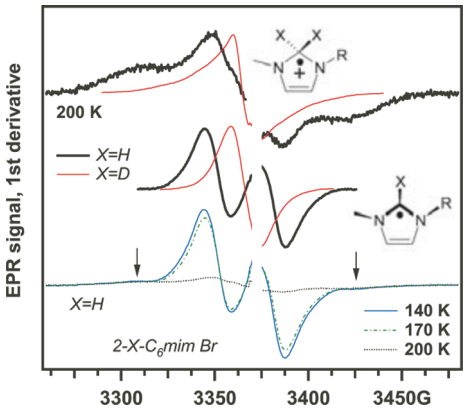


**Figure 1.** EPR spectra of irradiated frozen (vitreous) $h_3$ and $d_3$ isotopomers (2,4,5-$D_3$-substitution in the imidazolium ring) of $C_6$mim Br (bold lines for $h_3$ isotopomers). The spectra observed below 200 K exhibit the lines from the 2-imidazolyl, $Q_2X^{\bullet}$ radical, and its protonated form, $Q_2X_2^{+\bullet}$ (where X = H or D). The latter lines are indicated with arrows. Warming of the sample to 200 K causes the decay of $Q_2X^{\bullet}$. Subtracting the spectra obtained at 140 and 170 K yields the spectra from $Q_2X^{\bullet}$ (the middle two traces). The residual species observed at 200 K are $Q_2X_2^{+\bullet}$ (at the top). Here and in other figures the temperature is indicated in the plot.

(1 Gy = 1 J/kg) using 3 MeV electrons from Argonne's Van de Graaff accelerator.

**2.2. Room Temperature Radiolysis and Product Analyses.** In addition to low-temperature EPR experiments, radiolysis of ILs was carried out using the same 3 MeV electron beam. Liquid samples were placed into 10 mm diameter thin-wall glass tubes immersed into flowing chilled water. Due to poor heat conductivity of the ILs, the temperature of the sample increased to 60 °C during the electron beam radiolysis at 1.8 $\mu$A, using 12 ns electron pulses at 360 Hz. This temperature increase makes the IL less viscous, allowing the escape of radiolytically generated gases. Fricke dosimetry carried out using 5−50 pulses of 5 nC at the rate of 1 Hz indicated a dose rate of 678 Gy/s for 1 $\mu$A current (this dose was adjusted for the electron density of the IL).

Nuclear magnetic resonance (NMR) spectra were obtained in dimethyl sulfoxide-$d_6$ (DMSO), using an Avance DMX 500 MHz spectrometer (Bruker); the chemical shifts are given vs tetramethylsilane. Tandem electrospray ionization mass spectra ($ESMS_n$) were obtained using a Thermo Scientific LCQ Fleet ion trap mass spectrometer operating in either positive or negative modes ($MS_n^{\pm}$) using a spray voltage of 4.38 kV. $MS_1$ corresponds to the first quadrupole and $MS_2$ corresponds to collision induced dissociation mode of operation. Liquid samples were injected in dilute methanol solutions. The operating conditions were similar to those given in refs 1 and 4.

## 3. RESULTS

This section is organized as follows: In section 3.1 we consider several aspects of radiation chemistry for imidazolium cations, first considering the EPR spectroscopy results for frozen ILs and then ESMS and NMR results for ILs irradiated at room temperature. In section 3.2 these observations are extended to 2-alkyl-substituted imidazolium cations. In section 3.3 we compare these imidazolium cations to 1-butyl-4-methylpyridinium, which serves as a reference aromatic cation.

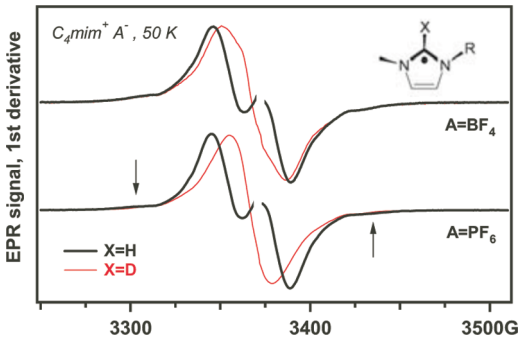


**Figure 2.** EPR spectra of 2-imidazolyl radicals for $h_3$ and $d_3$ isotopomers of $C_4$mim $BF_4$ and $C_4$mim $PF_6$ (Table 1S, Supporting Information). The side lines are indicated by arrows.

**3.1. Imidazolium Cations.** *3.1.1. 1-Methyl-3-alkylimidazolium ($C_n$mim$^+$): Formation of 2-Imidazolyl and R$^{\bullet}$($C^+$) Radicals.* We begin our examination by considering experimental evidence for the formation of the 2-imidazolyl radical in reaction 3. The principal difficulties in EPR studies of irradiated ILs are 2-fold: (1) resonance lines from many radicals (derived from both cations and anions) spectrally overlap, and (2) there is considerable secondary radical chemistry. Considering these challenges, $C_6$mim Br is a particularly convenient candidate for study, as reaction 2 produces Br$^{\bullet}$ atoms that cannot abstract H from the aliphatic arms of the cation (reaction 8) and therefore form $Br_2^{-\bullet}$ anions that have a highly anisotropic $g$-factor (see part 1).[1] Consequently, there is almost no spectral overlap between the organic radicals and this radical anion. Figure 1 exhibits the central part of the EPR spectrum at $g \approx 2$ for two isotopomers: $d_3$ and $h_3$ (hereafter, $d_3$ refers to deuteration of the 2, 4, and 5 positions of the imidazolium ring; see Table 1S, Supporting Information). The 50 K trace is composite: a narrower resonance line is superimposed on the broad 200 K signal; by double integration this broad line accounts for 60% of the radical yield (Figure 1). The progenitor of this narrow resonance line decays at 200 K. Subtracting the 200 K trace from the 175 K trace yields the two traces shown at the center of Figure 1. For the $h_3$ isotopomer, it is a doublet, whereas for the $d_3$ isotopomer, it is a narrow singlet. Qualitatively, this is consistent with a $Q_2H^{\bullet}$ $\sigma$-radical having a large (20−25 G) isotropic hyperfine coupling constant (hfcc) in H(2). The deuteron substitution in the 2-position collapses the EPR line as other hfcc's in this radical are rather small, whereas the spin-1 deuteron has only ≈15% of the magnetic moment of the spin-1/2 proton (Table 2S, Supporting Information). Our simulations of the EPR spectra from $Q_2H^{\bullet}$ with the parameters calculated using density functional theory (DFT) yield just such a pattern (Table 3S and Figures 1S, Supporting Information), and we identify this characteristic EPR spectrum and its transformation upon H(2) substitution as the signature of the 2-imidazolyl radical. The broad underlying triplet with the side lines separated by ∼100 G also collapses to a singlet upon deuteration in the imidazolium ring. As only the 2-protons in $Q_2H_2^{+\bullet}$ have hfcc's of sufficient magnitude, this feature (despite the lack of spectral resolution) can be confidently attributed to protonated $Q_2H^{\bullet}$ (see section 3.1.4 for further discussion of this radical identity).

Another such convenient system is $C_4$mim $PF_6$. As shown in ref 1, hexafluorophosphate does not yield radicals that are stable above 50 K. The EPR spectra from the $h_3$ and $d_3$ isotopomers

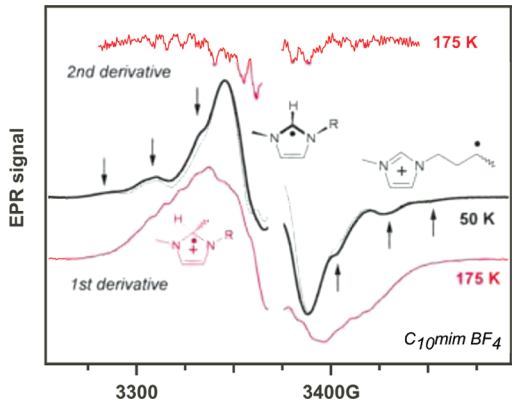


**Figure 3.** First derivative EPR spectrum of $C_{10}$mim $BF_4$ obtained at 0.02 mW (dashed line) and 2 mW (bold line). The microwave saturable signal is from the $Q_2H^{\bullet}$ radical, the less saturable signal is from the $R^{\bullet}(C^{+})$ radical, revealing the 25 G pattern of lines indicated by arrows. Warming of this sample causes the decay of these radicals and the gradual appearance of the line of $Q_2HR'^{+\bullet}$, which is fully resolved at 175 K. The second derivative EPR spectrum (at the top) reveals the characteristic 7 G pattern of lines typical of $Q_2HR'^{+\bullet}$ radicals.

look nearly identical to the spectra of 2-imidazolyl observed in irradiated $C_6$mim Br (compare Figures 1 and 2). When the $h_3$ sample is warmed to 180−200 K, a multiplet of lines spaced by ∼7 G is superimposed on top of the incompletely decayed signal of $Q_2HR'^{+\bullet}$ (Figure 2S(a), Supporting Information) The second-derivative EPR spectrum obtained at 180 K looks very similar to such spectra for $Q_2H_2^{+\bullet}$ in other systems (section 3.1.4). For the $d_3$ isotopomer (Figure 2S(b), Supporting Information), this line collapses to a broad, unresolved singlet that persists at 200 K. The narrow line spectrum shown in Figure 2b was obtained by the subtraction of the EPR spectra obtained at 160 and 180 K from each other, as only the $Q_2D^{\bullet}$ radical decays in this temperature interval. Decomposing the 50 K traces into signals from $Q_2D^{\bullet}$ and $Q_2D_2^{+\bullet}$ radicals (Figure 2S(b), Supporting Information) indicates that the latter accounts for ∼70% of the radical yield. Similar spectral transformations were observed for $C_4$mim $BF_4$ in Figures 2 and $C_2$mim $BF_4$ in Figure 3S(a) (Supporting Information) (the tetrafluoroborate also does not yield observable radicals from 50 to 200 K); however, due to the ease of hydrolysis of tetrafluoroborate, the H(2) proton exchange was only 50%, which resulted in incomplete collapse of the 2-imidazolyl doublet. The spectra for 2-imidazolyl radicals derived from $C_n$mim$^+$ are virtually identical for $n$ = 2 and $n$ = 4. In addition to the presence of 2-imidazolyl, two broad lines (indicated by arrows in Figure 2) separated by ∼115 G are prominent. Warming the irradiated $C_4$mim-$h$(2) $BF_4$ to 160 K produces a spectrum in which these resonance lines are better resolved (Figure 3S(b), Supporting Information). The same multiplet, with the apparent 25 G splitting typical of alkyl radicals, is observed in $d$(2)-substituted $C_2$mim $BF_4$, which has less spectral overlap between these resonance lines and 2-imidazolyl-$d$(2) (Figure 3S(b), Supporting Information). Since deuteration in the ring does not affect this multiplet, it can only be from (i) $R^{\bullet}$ radicals generated via reactions 13b and/or 14 or (ii) $R^{\bullet}(C^{+})$ radicals generated via reactions 4 and/or 8 (see Scheme 1). In Figure 3S(b) (Supporting Information) we plotted the simulated EPR spectra of ethyl and α-H and $\beta$-H loss $R^{\bullet}(C^{+})$ radicals assuming free rotation of the arm. Neither one of these radicals by itself can account for the 160 K spectrum,

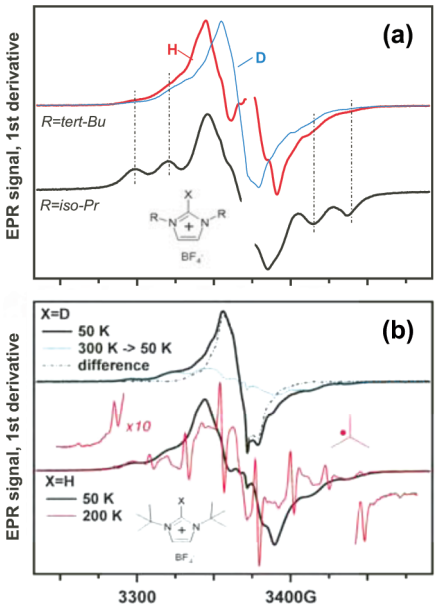


**Figure 4.** (a) EPR spectra for the $d_3$ and $h_3$ isotopomers of 1,3-di(*tert*-butyl)imidazolium tetrafluoroborate (marked in the plot H and D, respectively) compared to the EPR spectrum from 1,3-di-(isopropyl)imidazolium tetrafluoroborate. The lines from the alkyl radical are indicated with dash-dot lines. (b) At the bottom: warming of the 1,3-di(*tert*-butyl)imidazolium tetrafluoroborate above 170 K causes the gradual emergence of the $^{\bullet}CMe_3$ radical whose narrow lines are superimposed on the broader lines of the $R^{\bullet}(C^{+})$ radical. The latter persists at 300 K. At the top: the difference of EPR spectra for the $d_3$ isotopomer, one obtained at 50 K and another for a sample warmed to 300 K and then cooled back to 50 K, produces the narrow line of the $Q_2D^{\bullet}$ (dash-dot line).

but a combination of the two $R^{\bullet}(C^{+})$ radicals would account for the features observed.

Formation of such alkyl radicals becomes even more apparent for $C_n$mim$^+$ cations with long aliphatic arms. Figure 3 exhibits the spectrum obtained for irradiated $C_{10}$mim $BF_4$. The six lines indicated with arrows are separated by 25 G and can only be from the interior alkyl radical. Warming this sample above 160 K (Figure 3) results in the decay of these six lines; only then does the characteristic 7 G multiplet of lines from $Q_2HR'^{+\bullet}$ (see section 3.1.4) appear. Importantly, regardless of the position of the methyl group (1, 2, or 3) we never observed a four-line signal from methyl radicals, though such EPR patterns from methyl radicals can be easily produced in ILs containing acetate (which undergoes oxidative fragmentation to $^{\bullet}CH_3$ and $CO_2$).[1] Our data establish that *if a methyl radical is eliminated from the parent cation in any of the positions on the imidazolium ring, it must be a very rare occurrence.*

*3.1.2. Substituting Groups Other Than n-Alkyl: Elimination of Side Groups.* Since distinguishing between the $R^{\bullet}$ and $R^{\bullet}(C^{+})$ radicals for imidazolium cations with long aliphatic arms is problematic, as these two radicals have similar EPR spectra, we sought a more clear-cut example. To this end, we examined $h_3$ and $d_3$ isotopomers of 1,3-di(*tert*-butyl)imidazolium tetrafluoroborate, which is a crystalline solid. The main feature in the EPR spectrum of this irradiated solid (Figure 4a) was a doublet from the $Q_2H^{\bullet}$ radical, which collapsed to singlet upon deuterio substitution. As this radical is missing additional hyperfine coupling constants in the α-protons in the arms (see Table 3S, Supporting Information), the envelope of this line is narrower

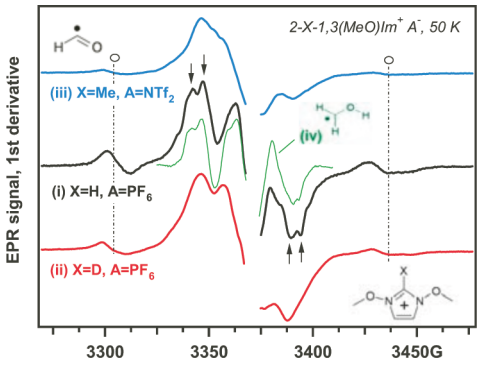


**Figure 5.** EPR spectra of (i) $h_3$ and (ii) $d_3$ isotopomers of 1,3-dimethoxyimidazolium hexafluorophosphate. The lines of the formyl radical, HC$^{\bullet}$O, are indicated with dash-dot lines and open circles. The split $M = \pm 1$ lines from the hydroxymethyl radical, $^{\bullet}CH_2OH$, are indicated with arrows. Trace (iii) exhibits the EPR spectrum of 2-methyl-1,3-dimethoxyimidazolium bistriflimide. In traces (ii) and (iii), the lines of the hydroxymethyl radical are also present, but poorly resolved at 50 K. Warming of the sample makes these lines fully resolved, as shown in trace (iv) (also see the captions to Figures 6S and 7S, Supporting Information).

than for 2-imidazolyl radicals of $C_n mim^+$. It is seen that this line spectrally overlaps with a signal whose outer lines indicate the 25 G pattern of an alkyl radical (indicated with dashed lines in Figure 4a). The same features are also observed in the $d_3$ isotopomer, supporting this attribution. Warming the $d_3$ sample to 300 K and observing the EPR spectrum at 50 K produces a six-line spectrum that can be attributed to an isopropyl radical in one of the arms (see the simulations in Figure 4S, Supporting Information). The same radical is observed in radiolysis of 1,3-di(isopropyl)imidazolium tetrafluoroborate, where it yields the largest contribution to the spectrum, overwhelming the weaker signal from 2-imidazolyl (Figure 4a and Figure 4S, Supporting Information). When the irradiated sample of 1,3-di(*tert*-butyl)imidazolium tetrafluoroborate is warmed above 125 K, the dectet narrow lines from $^{\bullet}C(CH_3)_3$ gradually appears (together with a much weaker signal from $Q_2H_2^{+\bullet}$), while the signal from $Q_2H^{\bullet}$ gradually disappears (Figure 4b). This behavior provides unambiguous evidence for reaction 14. Similar behavior was observed for 1,3-di(isopropyl)imidazolium tetrafluoroborate, where the lines of $Q_2HR'^{+\bullet}$ are better resolved (Figure 4S, Supporting Information). Unfortunately, the similarity of EPR spectra from $Q_1^{+\bullet}C(CH_3)_3$ and $^{\bullet}CH(CH)_3$ under the conditions of hindered rotation (see calculated magnetic parameters in Table 2S, Supporting Information) does not exclude the formation of R$^{\bullet}$, and the observation of 2-adduct $Q_2HR'^{+\bullet}$ at 160 K suggests that a small, mobile radical R$'^{\bullet}$ adds to the parent cation. This mobile radical could be the residue R$^{\bullet}$.

In the gas phase, collisionally activated imidazolium cations lose their aliphatic arms through reaction 13a.[19] No loss of methyl radicals from the 1-, 2-, or 3-positions was found in our $MS_2^+$ spectra for any of the cations studied. DFT calculations suggest that reaction 13a requires less activation than reaction 13b. For example, for $C_2mim^+$, the corresponding energy barriers are 1.17 and 4.4 eV. Turning to reaction 14, the dissociation energy of the N$-$CH$_3$ bond is only 77 meV, even for 1,3-dimethyl-2-imidazolyl; i.e., the $Q_3R^{\bullet}$ radicals are thermodynamically unstable. The alkyl substitution at $C_\alpha$ further reduces this energy, facilitating reaction 14.

Further weakening of the N$-$R bond can be achieved by replacing the alkyl arm with the alkoxy arm. In the $MS_2^+$ spectra for 1,3-dimethoxy substituted 2-*R*-imidazolium cations (R = H or CH$_3$; Figure 5S(a), Supporting Information), there are major mass peaks corresponding to the loss of CH$_3$O, CH$_3$OH, RCN, and HC(O)NH$_2$ ($m/z$ 31, 32, 27, and 45), suggesting the occurrence of N$-$O scission in addition to ring rearrangement and contraction (Figure 5S(b), Supporting Information). For 1,3-dimethoxy-2-imidazolyl, reaction 14 is *exergonic* by 1.06 eV, while reactions 13a and 13b are endergonic by 1.29 and 2.36 eV, respectively. These estimates suggest the ease of losing the *N*-methoxy arms.

In Figure 5, we examine EPR spectra observed for irradiated, crystalline $h_3$ and $d_3$ 1,3-dimethoxyimidazolium hexafluorophosphate and 2-methyl-1,3-dimethoxyimidazolium bistriflimide. These EPR spectra exhibit two doublets of lines (marked with empty circles in Figure 5) that are absent in other ILs. The splitting of these two lines (126 G) corresponds to a rotating formyl radical, H$^{\bullet}$CO. In addition to this doublet, there are split $M = \pm 1$ lines from α-protons in the $^{\bullet}CH_2OH$ radical generated via rearrangement of the leaving CH$_3$O$^{\bullet}$ radical (indicated with the arrows in the plot). These lines become fully resolved at 100$-$150 K for both $h_3$ and $d_3$ isotopomers of 1,3-dimethoxyimidazolium (Figures 6S and 7S, Supporting Information). Above 200 K, the resonance lines of the H$^{\bullet}$CO and $^{\bullet}CH_2OH$ radicals disappear, while a broad line of some other radical remains, persisting to 300 K. Upon $d_3$ substitution in the ring, this line narrows, exhibiting some resolved structure, overlapping with the residual $^{\bullet}CH_2OH$ (Figure 8S, Supporting Information). This persistent EPR signal can be subtracted from the EPR spectra obtained at lower temperature and the presence of the $^{\bullet}CH_2OH$ becomes apparent in such difference spectra (Figure 5, trace iv). Comparison to the simulated spectrum of $Q_3^+(OCH_2^{\bullet})$ excludes this radical as the progenitor of the observed spectrum.

The methoxy radical (which is the precursor of $^{\bullet}CH_2OH$) can be formed via either reaction 13b or 14 (see Scheme 1S, Supporting Information). In the latter case, the $Q_3^{+\bullet}$ radical cation is also generated. This is a $\pi$-radical with large hfcc's for the H(2) and H(5) protons (Table 2S, Supporting Information). The EPR spectrum of this radical collapses to a narrower line in the $d_3$ isotopomer (Figure 8S, Supporting Information, to the top). Such a transformation was observed in the high-temperature line (Figure 8S, Supporting Information), although the agreement between the observed and the simulated spectra is rather poor (partially, due to the strong spectral overlap), and we tentatively identify the persistent radical with $Q_3^{+\bullet}$. The latter is a known intermediate[20] in cathodic polymerization of imidazole that yields an N$-$N bound dimer, $(Q_3)_2^{2+}$ (Scheme 1S, Supporting Information). The formation of the formyl radical and the absence of the $Q_3^+(OCH_2^{\bullet})$ radical (generated in reaction 4) can be accounted for by energetics. DFT calculations indicate that the -H radical formed in reaction 4 would be unstable, dissociating to formaldehyde and $Q_3^{+\bullet}$:

$$Q_3^+(OCH_2^{\bullet}) \rightarrow Q_3^{+\bullet} + CH_2O \qquad (15a)$$

If the latter radical cation abstracts H from formaldehyde,

$$Q_3^{+\bullet} + CH_2O \rightarrow Q_3H^+ + H^{\bullet}CO \qquad (15b)$$

one obtains the formyl radical (Scheme 1S, Supporting Information). In the gas phase, reactions 15a and 15b are exergonic

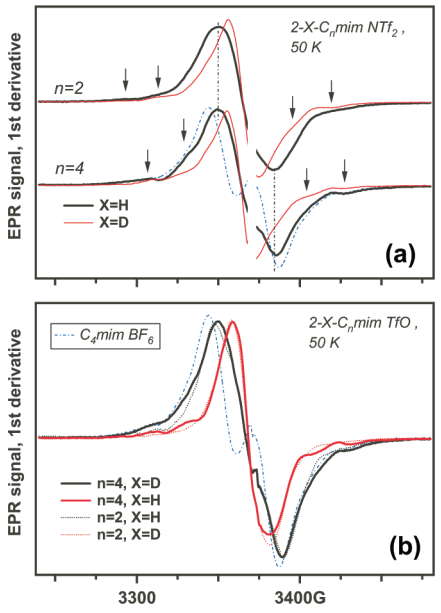


**Figure 6.** EPR spectra from irradiated $C_n$mim ($n$ = 2, 4) bistriflimides (a) and triflates (b). Both the $h_3$ and $d_3$ isotopomers are shown, and the lines of $R^{\bullet}(C^{+})$ are indicated with arrows. In both panels, the spectrum of the 2-imidazolyl observed in $C_4$mim $BF_4$ is shown for comparison (dashed line).

by 0.06 and 0.91 eV, respectively (these two reactions could be concerted). Thus, in *N*-methoxy substituted imidazolium cations, the loss of the methoxy arm ensues in both reactions 2 and 3.

Another example of atypical but illuminating chemistry is provided by the only zwitterionic compound we studied, which is 1,3-dimethylimidazolium-2-carboxylate (in our nomenclature, $Q_2^{+}(CO_2^{-})$). By analogy with other carboxylates,[1] we can expect oxidative decarboxylation

$$Q_2^{+}CO_2^{-} + h^{+\bullet} \rightarrow Q_2^{+\bullet} + CO_2 \qquad (16)$$

in addition to reaction 3 that yields the 2-substituted $Q_2(CO_2^{-})^{\bullet}$ radical. Our simulations (Table 2S and Figure 9S(a)), Supporting Information) indicate that $Q_2^{+\bullet}$ and $Q_2(CO_2^{-})^{\bullet}$ radicals have similar EPR spectra despite having rather different hfcc's, and both of these spectra compare well with the experimental spectrum observed in irradiated crystals of this compound. As the sample is warmed to 175−200 K, the overall envelope of the spectrum does not change, while the second-derivative EPR spectrum reveals the gradual formation of the $Q_2H_2^{+\bullet}$ (Figure 9S(b), Supporting Information'). A natural path to this radical (Scheme 2S, Supporting Information) is a two-step protonation of $Q_2(CO_2^{-})^{\bullet}$:

$$Q_2(CO_2^{-})^{\bullet} + H^{+} \rightarrow Q_2H^{\bullet} + CO_2 \qquad (17)$$

followed by reaction 10. The reactions of the $H^{\bullet}$ atoms would yield the 2-imidazolyl radical (reaction 18) or diamagnetic $Q_2H^{+}$ cation (reaction 19):

$$Q_2^{+}(CO_2^{-}) + H^{\bullet} \rightarrow Q_2H^{\bullet} + CO_2 \qquad (18)$$

$$Q_2^{+\bullet} + H^{\bullet} \rightarrow Q_2H^{+} \qquad (19)$$

Reaction 19 is unlikely given that it should compete with reaction 18, but without $Q_2H^{+}$, $Q_2H_2^{+\bullet}$ cannot be generated through reaction 10. Given that the $Q_2H_2^{+\bullet}$ radical is observed only at high temperature, whereas reactions 18 and 19 should occur even at low temperature, these observations (as well as the observations discussed below) strongly suggest that most of the $Q_2H_2^{+\bullet}$ radicals are produced via reaction 10 rather than reaction 9.

*3.1.3. C(2)−C(2) Dimer Cation Formation.* In all of the systems examined above, the product of electron attachment to the cation was the 2-imidazolyl radical $Q_2H^{\bullet}$, as opposed to the dimer radical cation $(Q_2H)_2^{+\bullet}$ (reaction 6). We also identified this monomer radical in ILs involving $(RO)_2PO_2^{-}$, $RSO_3^{-}$, and $ROSO_3^{-}$ anions. In the following, we refer to such IL systems as class I.

On the other hand, in class II liquids that are composed of $NTf_2^{-}$, $TfO^{-}$, and (with less confidence) $N(CN)_2^{-}$, the EPR spectra looked different. As discussed in ref 5, the EPR signature of $(Q_2H)_2^{+\bullet}$, as opposed to $Q_2H^{\bullet}$, is narrowing of the spectral envelope and disappearance of the doublet structure (as the spin density is shared by both monomer units). In class I systems, this doublet structure is clearly resolved, and the field interval between the points of maximum slope ($\Delta B_{pp}$) is ≈45 G. For $NTf_2^{-}$, $TfO^{-}$, and $N(CN)_2^{-}$ (not shown) this $\Delta B_{pp}$ is only ≈36 G and the doublet structure is absent (Figure 6a,b). Yet the observed radical undergoes the same narrowing to a narrow singlet line upon $d_3$ substitution. Furthermore, almost identical spectra are obtained for $C_2$mim$^{+}$ and $C_4$mim$^{+}$ (Figure 6b), suggesting that the radical does not have strong couplings to $\beta$-protons in the arms. To estimate the effect of α-protons, we synthesized isotopomers of $C_4$mim $NTf_2$ with (i) $CD_3$ and (ii) *n*-$C_4D_9$ arms (section 1S and Figure 10S(a), Supporting Information) and isotopomers of $C_2$mim $NTf_2$ with (i) $CH_2CH_3$, (ii) $CH_2CD_3$, and (iii) $CD_2CH_3$ arms (section 1S and Figure 10S(b), Supporting Information). Comparison of the EPR spectra from the three isotopomers of $C_2$mim $NTf_2$ shows almost no significant difference in their spectra, suggesting weak coupling to the α-protons. Both H/D substitutions in $C_4$mim $NTf_2$ produced some difference, but the main difference was not an effect on the EPR signal of interest, but rather the formation of narrow lines superimposed onto this signal without changing the latter. As there is a concomitant disappearance of the lines in the spectral wings that we attribute to $R^{\bullet}$ or $R^{\bullet}(C^{+})$ radicals (section 3.1.1), the effect of deuteration was solely the production of deuterated analogs of such radicals, yielding this narrow signal. The presence of such $R^{\bullet}$ or $R^{\bullet}(C^{+})$ radicals can be inferred by warming the samples to 160−180 K, when the lines of the alkyl radicals become more discernible, as other radicals decay. The import of these H/D substitution experiments is that the effect of such substitution on the main spectral feature is minor. These observations leave only one explanation of the class II spectra: the narrow singlet arises from the dimer radical cation, so reaction 6 is shifted to the right side in these class II systems. Another finding from these H/D substitution experiments is indirect proof of deprotonation reaction 4 involving the short arm of $C_n$mim$^{+}$ (as a minor reaction channel).

Warming of class I systems always results in the formation of $Q_2H_2^{+\bullet}$. The salient feature of class II systems is that warming of the samples does not yield $Q_2H_2^{+\bullet}$ except when these samples are intentionally hydrated. The typical temperature dependences for bistriflimides and triflates are shown in Figures 11S and 12S, Supporting Information. While the EPR spectrum changes considerably, exhibiting the stronger signal from $R^{\bullet}(C^{+})$ (marked with open circles) and a narrow feature from $^{\bullet}CF_2\sim$ (fragment) radicals (marked with an arrow), the characteristic 7

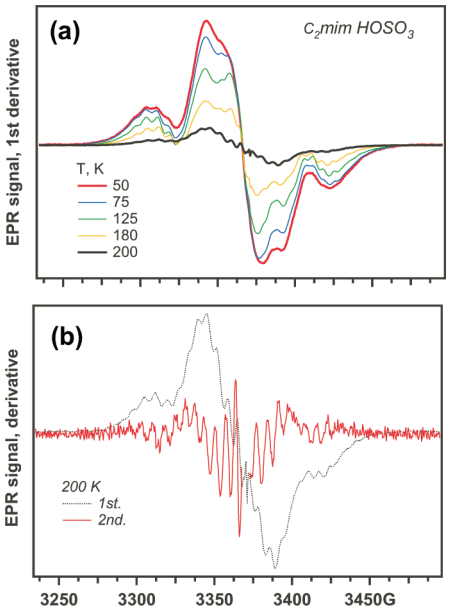


**Figure 7.** (a) Temperature dependence of EPR spectra from irradiated $C_2$mim $HSO_4$ and (b) the fully resolved first and second derivative EPR spectra of $Q_2H_2^{+\bullet}$ at 200 K.

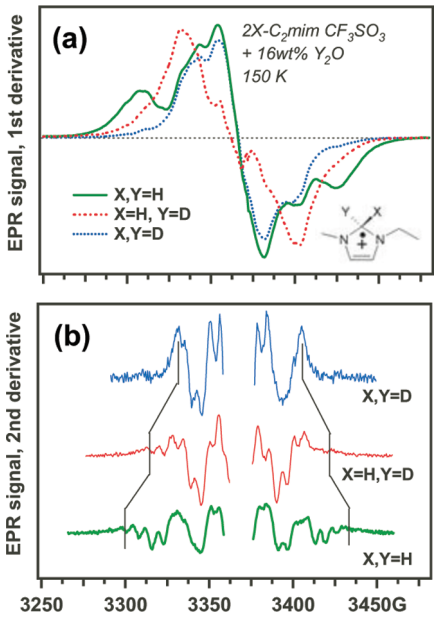


**Figure 8.** (a) First derivative EPR spectra of the irradiated $h_3$ and $d_3$ isotopomers of $C_2$mim TfO containing 16 wt % $H_2O$ or $D_2O$ (see the legend in the plot). Panel b exhibits the corresponding second derivative EPR spectra that reveal the 7 G pattern of the resonance lines of the $Q_2XY^{+\bullet}$ radical cations (X, Y = H, D).

G multiplet of the lines from $Q_2HR'^{+\bullet}$ radicals is not observed, and there is no change upon deuteration (see the comparison in Figure 13S, Supporting Information). The residual signal in $C_n$mim $NTf_2$ is very similar to $R^{\bullet}(C^{+})$ in irradiated $HNEt_3$ $NTf_2$ (shown in Figure 13S, Supporting Information)[4] As discussed in sections 3.2 and 3.3, such protonation was not observed for 2-methylimidazolyl and 4-methylpyridyl radicals. The logical explanation of these observations is that substitution at C(2) prevents reaction 10. The 2-imidazolyl radical in class I liquids can be readily protonated at C(2). The dimer radical cation in class II liquids, $(Q_2H)_2^{+\bullet}$, cannot be protonated as it is substituted at the accepting site. In these class II liquids, only reaction 9 can produce the $Q_2HR'^{+\bullet}$ radicals. This requires abundant protic impurities.

In ref 5, we speculated that $(Q_2H)_2^{+\bullet}$ can deprotonate,

$$(Q_2H)_2^{+\bullet} + A^- \rightarrow Q_2(Q_2H)^{\bullet} + H^+A^- \qquad (20)$$

yielding the $Q_2$-substituted 2-imidazolyl radical. The latter species has an EPR spectrum resembling that of $Q_2H^{\bullet}$, as H(2) in $Q_2H^{\bullet}$ and $\beta$-H in $Q_2(Q_2H)^{\bullet}$ have comparable hfcc's (25.5 G vs 15.8 G, Table 3S, Supporting Information). The congested EPR spectra did not allow us to establish whether reaction 20 takes place in Class II liquids.

*3.1.4. Protonated 2-Imidazolyl.* The issue of H atom addition and protonation equilibria already came up in preceding sections. While we have repeatedly identified certain patterns as arising from $Q_2HR'^{+\bullet}$ radical cations, no proof of this identification has been provided so far. In this section, we establish the identity of the progenitor of this spectrum.

The calculated hfcc parameters for the $Q_2HR'^{+\bullet}$ are given in ref 7 and Table 4S (Supporting Information). The only substantial hfcc's in the 2-substituting groups (R) are found for R = H (~41 G), −R = $^{19}$F (83 G), and R = $^{14}NR_2$ (6−9 G, depending on substitution), i.e., only when the magnetic nucleus is in the α-position to C(2). Because hfcc's for $^{14}$N(1,3), $^{1}$H(4.5), and α-protons in the aliphatic arms are 6.5−7.5 G for all $Q_2HR'^{+\bullet}$ radicals, the latter (for R having no magnetic α-nuclei at C(2)) exhibit EPR spectra similar to the $Q_2HD^{+\bullet}$ radicals, and the $Q_2XR'^{+\bullet}$ radicals exhibit EPR spectra similar to the $Q_2D_2^{+\bullet}$ radicals. All of these spectra exhibit the characteristic 7 G pattern. Simulated EPR spectra for these three isotopomers are shown in Figure 14S (Supporting Information). As the same species is produced in reaction 9 or 10, one can generate this radical cation by generating $H^{\bullet}$ or $D^{\bullet}$ atoms.

Such a possibility is presented in $C_2$mim $HOSO_3$, as the $H^{\bullet}$ atoms are generated via dissociative electron attachment to the anion,

$$HOSO_3^- + e^{-\bullet} \rightarrow H^{\bullet} + SO_4^{2-} \qquad (21)$$

The resulting EPR spectrum is shown in Figure 7a. The side lines correspond to the weak lines indicated with arrows, previously introduced in Figures 1 and 2. A 7 G pattern is discernible even at 50 K. At higher temperature, it becomes fully resolved. Figure 7b exhibits the second-derivative EPR spectrum of the 200 K trace, in which all resonance lines of the $Q_2H_2^{+\bullet}$ radical are resolved.

Another approach uses water as the source of the protons and the $H^{\bullet}$ atoms. As $C_4$mim $CF_3SO_3$ is a class II liquid (section 3.1.3), irradiation of the neat IL does not yield the $Q_2H_2^{+\bullet}$ radical. However, by addition of 5−50 wt % $H_2O$ (triflate ILs are water miscible), $H^{\bullet}$ atoms can be produced with good yield. The EPR spectra observed at 50 K are complex, but at 150−200 K, the adduct radical cations impart the main observed feature. A typical spectrum transformation is shown in Figure 15S (Supporting Information). The lines of the $Q_2H_2^{+\bullet}$ are already apparent at 50 K; at 150 K, the spectrum is fully resolved. For comparison, we overlaid the EPR spectrum observed in irradiated 1,3-dimethyimidazolium dimethylphosphate at 205 K. While both EPR spectra reveal a 7 G pattern typical of the C(2) adducts, it is seen that in one case the EPR spectrum is a triplet, whereas in the other it is a doublet. This difference

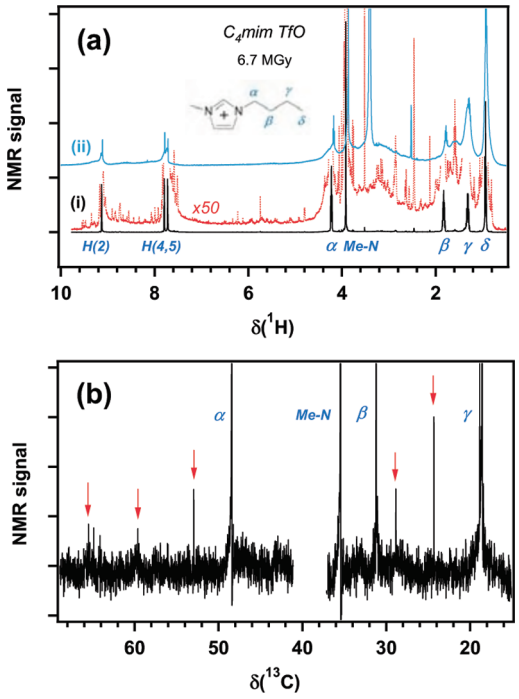


**Figure 9.** (a) $^{1}$H and (b) $^{13}$C NMR spectra of $C_4$mim TfO irradiated to 6.7 MGy. The irradiated sample exhibits broad resonance lines at 2−4 ppm (trace i). Trace ii is the NMR spectrum of water insoluble fraction of the irradiated IL diluted in DMSO-$d_6$. In panel b the signal from the solvent is not shown. The arrows indicate the resonance lines that are absent in the sample before irradiation.

indicates that in one case the C(2) adduct is the $Q_2H_2^{+\bullet}$ radical, whereas in the second case it is a $Q_2HR'^{+\bullet}$ radical.

This difference can be made visible in an experiment involving $h_3$ and $d_3$ isotopomers of $C_2$mim TfO (the sample contains 16 wt % $D_2O$). As the irradiation of $D_2O$ produces $D^\bullet$ atoms, reaction 9 produces

$$D^\bullet + Q_2H^+ \rightarrow Q_2DH^{+\bullet} \quad (22)$$

or

$$D^\bullet + Q_2D^+ \rightarrow Q_2D_2^{+\bullet} \quad (23)$$

The EPR spectra obtained at 200 K are shown in Figure 8a,b. The anticipated $Q_2H_2^{+\bullet}$ exhibits a broad triplet collapsing to a doublet (for $Q_2HD^{+\bullet}$, reaction 22) collapsing to a singlet (for $Q_2D_2^{+\bullet}$, reaction 23) The second derivative EPR spectrum in Figure 8b reveals the 7 G patterns for all three of these radicals, and the width of the EPR spectrum corresponds to that expected for the three isotopomers. This demonstration completes our proof.

While it is, generally, impossible to establish the nature of the substituting groups X and R′ at carbon-2 in the $Q_2XR'^{+\bullet}$ for groups other than −H, the identification of this radical and establishing the degree of substitution at C(2) are straightforward from the data presented. This ability allowed us to infer protonation and C(2)-addition radical reactions in both parts of our study.

*3.1.5. NMR and ESMS Analyses of Irradiated ILs.* To obtain more insight in the radiation chemistry of $C_nmim^+$ cations, we carried out studies of stable radiolytic products (section 2.2). The viscosity of the irradiated IL samples increases considerably after

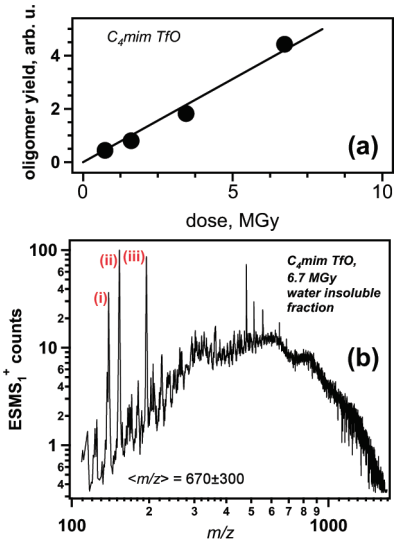


**Figure 10.** (a) Integrated $ESMS_1^+$ ion counts from the oligomer (normalized by the signal from the cation) as the function of dose in the irradiation of $C_4$mim TfO. (b) $ESMS_1^+$ spectrum from the water insoluble polymer generated in the radiolysis of $C_4$mim TfO to the total dose of 6.7 MGy. The mass peaks i, ii, and iii correspond to the parent cation and its 2-methyl and 2-butyl derivatives. The broad peak is from the oligomer with a mean $m/z$ of 670 ± 300. Note the logarithmic scale for both axes.

exposure to 0.5−2.0 MGy,[21] suggesting ongoing polymerization, and there is significant evolution of gas.[18,22]

The $^{1}$H NMR spectra of $C_4$mim TfO and $C_5$mim $NTf_2$ exposed to 6−8 MGy indicate ∼30% loss of α- and β-hydrogens from the long aliphatic arm (Figure 9a and Figure 16S, Supporting Information, respectively). There are also weak resonance lines that appear at 2.2−3.5 ppm (Figure 9a). Concomitant with these changes in the $^{1}$H NMR spectra is the appearance of new lines in the $^{13}$C NMR spectra at 24, 28, 53, 60, and 66 ppm, at ∼1−10% of the cation concentration (Figure 9b). Cross recombination of $R^\bullet(C^+)$ radicals and polymerization of olefinic products of their disproportionation would yield products exhibiting such NMR spectra. Oligomerization is suggested not only by a viscosity increase and these NMR spectra but also by $MS_1^+$ spectra (Figure 17S, Supporting Information): in addition to sharp mass peaks of $C^+$ and $C_2A^+$ ions, there is a diffuse continuum of mass peaks (with individual ion counts <1% of the $C^+$ mass peak) stretching out to $m/z$ 1700. The integral under this continuum linearly increases with the radiation dose (Figure 10a). A mean $m/z$ of 600 ± 300 was obtained for both of the ILs. When the irradiated $C_5$mim $NTf_2$ (which is immiscible with water before irradiation) was contacted with $D_2O$ (1:5 w/w), the pH of the aqueous solution was 2.5, indicating radiolytic generation of acid (∼0.02 per 100 eV). The acidification of the ILs and generation of $-H_{\alpha,\beta}$ loss products is consistent with reactions 2 and 4. $^{1}$H NMR spectra of these $D_2O$ solutions indicated significant cation loss to the aqueous phase. The $MS_1^+$ spectrum of this solution was consistent with the $C_5mim^+$ cation, but the $MS_1^-$ spectrum revealed the 1:5 ratio for mass peaks with $m/z$ 149 and 280, suggesting that some $NTf_2^-$ anions were converted to $TfO^-$ during radiolysis. Fragmentation of hydrophobic $NTf_2^-$ anions readily accounts for the cation loss to the aqueous phase.

As $C_4$mim TfO is water miscible, we dissolved the irradiated sample in water and found that a fraction of the irradiated


dx.doi.org/10.1021/jp200305b |J. Phys. Chem. B 2011, 115, 3889–3902

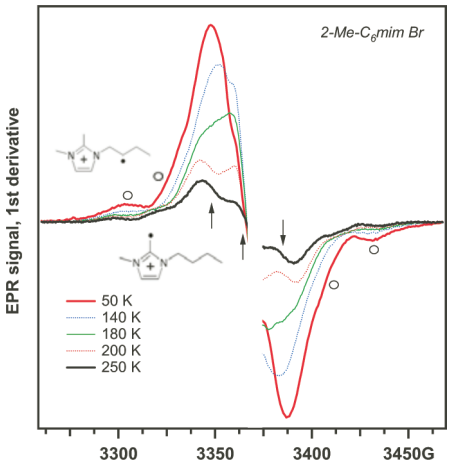


**Figure 11.** EPR spectra of irradiated 2-Me-$C_n$mim Br at several temperatures (indicated in the legend). The lines indicated with circles are from the $R^{\bullet}(C^{+})$ radical. The line at the center is mainly from the 2-methylimidazolyl radical. As the temperature increases, this radical decays and the EPR spectrum exhibits the triplet signature of $Q_2CH_2^{+\bullet}$. Notice the absence of the $Q_2HMe^{+\bullet}$ radical in these spectra. Arrows indicate a radical that persists to 300 K.

material was immiscible with water. This oily residue was washed with plenty of water and subsequently dried in a lyophilizer. The yield of this fraction from the sample irradiated to 6.7 MGy was 4.5 wt %. This residue readily dissolves in methanol and DMSO. The $^1$H NMR spectrum reveals a broad line between 2.3 and 4.4 ppm (Figure 9a) and additional lines overlapping with the sharp lines from the parent cation. It is apparent that broad NMR signals in the irradiated (unfractionated) ILs are from this water-insoluble polymer. In the $MS_1^+$ spectra of this residue (Figure 10b), there is a continuum of mass peaks between $m/z$ 100 and 1600, centered at $m/z$ 600 and accounting for 95% of the total ion counts (the average $m/z$ is 670 ± 300). Again, this is similar to the estimates for the polymer in neat $C_4$mim TfO (Figure 17S, Supporting Information). Against this continuum, there are mass peaks for $m/z$ 139 (the parent cation), 153 (2-methyl derivative), and 195 (2-butyl derivative), as suggested by the fragmentation patterns observed in the corresponding $MS_2^+$ spectra. The $MS_1^{\pm}$ spectra of the water-soluble fraction are identical to those for unirradiated $C_4$mim TfO.

The broad NMR signals, wide mass distribution, and low radiolytic yield (~0.23 monomer units per 100 eV) make it difficult to observe the polymer in the low-dose regime against the background of a much greater signal from the IL solvent, but its formation is clear from Figure 10a.

**3.2. 2-Methylimidazolium Cations (2-MeC$_n$mim$^+$).** Ionic liquids based on 2-alkylimidazolium cations ($Q_2X^+$) have certain advantages over more popular imidazolium cations under basic conditions, as the former cations cannot deprotonate from the 2-position, yielding $Q_2^{\bullet\bullet}$ and initiating a rich chemistry of its own, including dimerization and addition to the parent cation.[7,15] Shkrob[7] observed that similar products can also occur through the reactions of $Q_2H^{\bullet}$ and suggested that using $Q_2X^+$ cations can curtail this pathway to radiation damage. The occurrence of reaction 6 in class II liquids also indicates this negative tendency. Unfortunately, most of the presently used aromatic ILs are based on such unsubstituted imidazolium cations, and 2-methyl substitution has been shown to have the counterintuitive but nonetheless rationally explained[23] effect of raising IL viscosities and melting points. However, given the potential radiolytic advantages it is pertinent to ask what changes are observed when the imidazolium cations are substituted in their 2-position.

Irradiation of 2-Me-$C_6$mim Br yields the EPR spectrum shown in Figure 11. This spectrum consists of a central line with a peak-to-peak width of 45 G (at 50 K) and side lines. Increasing the temperature of the sample causes a rather complex spectral evolution, eventually yielding a radical that persists to 300 K without further evolution (the lines of this radical are indicated by arrows in Figure 11) and the $R^{\bullet}(C^{+})$ radical (open circles in the same plot). In Figure 18S (Supporting Information), we compare this "terminal" spectrum with the one obtained for chloride, triflate, tetrafluoroborate, and hexafluorophosphate of 1,2-dimethyl-3-butylimidazolium (also obtained at 200 K); these EPR spectra are similar (though not fully identical) and reveal the 25 G pattern of the alkyl radical. None of these EPR spectra exhibit the characteristic 7 G pattern of the $Q_2XH^{+\bullet}$ (X = H, R′) radicals that are so common for ILs composed of $Q_2H^+$ cations (section 3.1.4), and all of these exhibit the three-line patters shown in Figure 11. In addition to these ILs, we examined several 2-methylated bistriflimides, such as 1,2-dimethyl-3-propylimidazolium bistriflimide. Neither one of these ILs revealed the expected signals from the $Q_2(CH_3)H^{+\bullet}$ radicals. However, such radicals were observed in irradiated 1,2,3-trimethylimidazolium methylsulfate (Figure 19S, Supporting Information) and 2-methyl-1,3-dimethoxyimidazolium bistriflimide. Both of these systems yield hydroxymethyl radicals, the former through oxidative fragmentation of methylsulfate,[1] the latter through the elimination of the methoxy arms (section 3.1.2), so the adduct radical cations originate through secondary radical chemistry. We conclude that both reactions 9 and 10 are suppressed when the imidazolium cations are 2-methylated. The *alkyl substitution at C(2) reduces the proton affinity of the 2-imidazolyl radical, most likely through the introduction of steric hindrance.*

As demonstrated in part 1 of this study,[1] methyl radicals generated from oxidative decarboxylation of acetate readily form $Q_2(CH_3)H^{+\bullet}$ adducts at higher temperature, and one could expect that the same radical would be generated in reaction 9. Figure 9 and Figure 18S (Supporting Information) reveal a triplet (marked with the arrows in the plot) that likely originates from the $Q_2CH_2^{+\bullet}$ radical cation (Table 2S, Supporting Information). The same steric hindrance that opposes protonation of the $Q_2CH_3^{\bullet}$ at the accessible C(2) site leads to H-abstraction instead of H-addition in reaction with hydrogen atoms:

$$Q_2CH_3^+ + H^{\bullet} \rightarrow Q_2CH_2^{+\bullet} + H_2 \qquad (24)$$

The presence of $R^{\bullet}(C^{+})$ and $Q_2CH_2^{+\bullet}$ radicals results in strong spectral overlap with the $Q_2CH_3^{\bullet}$ radical. The latter has hindered rotation of its 2-methyl group, contributing to difficulty in interpreting the EPR spectra (Figure 1S, Supporting Information). At 50 K, this rotation is arrested in 2-Me-$C_4$mim $BF_4$ (Figure 20S, Supporting Information) and 2-Me-$C_4$mim $PF_6$ (Figure 21S, 'Supporting Information) yielding the EPR spectrum of $Q_2CH_3^{\bullet}$ and closely resembling that of $Q_2H^{\bullet}$ (see simulations in Figure 1S, Supporting Information). In other ILs, the "doublet" structure is missing as the methyl group is more freely rotating in the frozen matrix; in this case the EPR spectrum of $Q_2CH_3^{\bullet}$ becomes a singlet line (Figure 11). The same spectral transformation occurs in tetrafluoroborate and hexafluorophosphate when the temperature increases and the methyl group rotates more freely (Figures 20S and 21S, Supporting

**Scheme 2. Radicals Derived from 1-Alkyl-4-methylpyridinium, 1 ($C_n$MePy$^+$)**

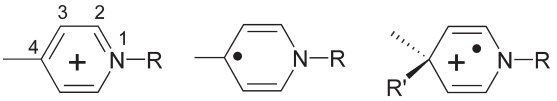


1 2 3

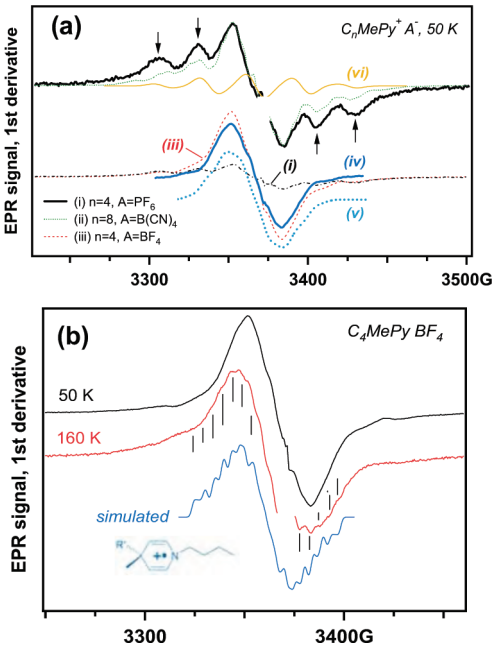


**Figure 12.** (a) EPR spectra from irradiated ILs composed of 1-alkylpyridinium cations. The structures corresponding to traces i, ii, and iii are indicated in the plot. Trace iv is spectrum iii from which scaled spectrum i was subtracted. This line is from radical **2**, as suggested by simulations (trace v). The lines indicated by arrows are from an $R^{\bullet}(C^+)$ radical. Comparisons to simulated spectra suggest that this is an alkyl radical generated by deprotonation from the α-position in the butyl arm of the oxidized cation. Panel b indicates changes in trace iii at higher temperature (160 K). The signal from $R^{\bullet}(C^+)$ disappears and a broad line exhibiting a 5 G multiplet pattern appears. Radical **3** would have just such a spectrum, where R′ is not a proton.

Information). These transformations are concomitant with the decay of this $Q_2CH_3^{\bullet}$ radical.

**3.3. 4-Methyl-1-butylpyridinium ($C_4MePy^+$).** Derivatized pyridinium cations, such as 4-methyl-1-butylpyridinium ($C_4MePy^+$, **1** in Scheme 2) provide another example of aromatic cations with improved chemical stability (as compared to 1,3-dialkylimidazolium). In analogy to the imidazolium cations, one may expect the occurrence of reaction 3, yielding a planar-ring C(4) centered $\pi$-radical **2** instead of a puckered-ring C(2) $\sigma$-radical for imidazolium (Scheme 2). Despite these structural differences, the hfcc of the $\beta$-protons in the 4-methyl group are comparable (9.2 G vs 11.7 G). Assuming free rotation of the 4-methyl group in **2**, the simulated EPR spectrum is a singlet with $\Delta B_{pp} \sim 34$ G (Table 5S, Supporting Information and trace v in Figure 12a). A line with $\Delta B_{pp} \approx 31$ G is observed in irradiated $C_4MePy\ BF_4$ (trace iii). This line is superimposed on the multiplet of lines from an alkyl radical (indicated with the arrows in the same plot). The presence of such alkyl radicals is apparent in the EPR spectrum of irradiated $C_4MePy\ PF_6$ (trace i) and also $C_8HPy\ B(CN)_4$ (trace ii), where the alkyl radical provides the main contribution (trace vi is the simulation of the corresponding α-radical; see Table 5S, Supporting Information). Subtracting scaled trace i from trace iii produces the spectrum of **2** (trace iv); the latter species accounts for 40% of the radical yield in irradiated $C_4MePy\ BF_4$. In analogy to reactions 9 and 10 for imidazolium cations, we anticipated $H^{\bullet}$ atom addition to **1** or protonation of **2**, both yielding **3**. The latter would appear as a broad doublet (Table 2S, Supporting Information) due to the large hfcc in the 4-proton (≈60 G). Since isotropic hfcc's for 3-protons and $^{14}N$ are ≈9 G, whereas α-protons in the 1-alkyl chain have hfcc's of ≈5 G, the simulated EPR spectra exhibit a distinctive 5 G pattern (Figure 12b). At 160 K, we observed the disappearance of the $R^{\bullet}(C^+)$ radical and the appearance of this 5 G pattern for irradiated $C_4MePy\ BF_4$; however, the spectral envelope corresponds to a $CR'^{+\bullet}$ rather than a $CH^{+\bullet}$ adduct (see the simulation in the plot), suggesting a secondary reaction with a fragment radical as opposed to reactions 9 and 10. For $C_4MePy\ PF_6$, such adduct radical cations were not observed.

While electron attachment reaction 3 is common for aromatic ILs, the protonation of the resulting radical, reaction 10, was observed only for unsubstituted imidazolium.

## 4. DISCUSSION

One of the concerns regarding ILs as next generation solvents for nuclear cycle separations is that continuous irradiation of these ILs by decaying radionuclides would result in the formation of metal-binding derivatives, volatilization, an increase in their viscosity, and changing proticity. Radiolytic degradation of the solvent is a common concern in the design of new extraction processes for radionuclide separations.[4,6,24,25] For example, radiolytic decomposition of the common metal extracting agent, tributylphosphate (with the $G$ value of ∼1.0/100 eV), by elimination of the butyl group and the formation of di- and monobutyl phosphoric acids (that nonspecifically bind to lanthanide ions), is one of the major complications in the PUREX process for U/Pu separations.[24]

Radiolytic damage to the ionic components of the ILs can be quite extensive as doses increase.[17] For imidazolium liquids, the radiolytic yields for decomposition of the cations are ∼2.8 per 100 eV for $C_4mim\ NTf_2$ and ∼3.7 per 100 eV for $C_4mim\ TfO$, respectively.[18] For a dose of 0.1−1 MGy (accumulated by the extraction solvent over its lifetime),[18] 5−10% of the cations may decompose. The most detrimental products (from the standpoint of metal extraction) are derived from the constituent *anions* that decompose with $G$ values of 1.0−2.1/100 eV; however, some of these products (including flammable $H_2$, which is generated at 0.26 per 100 eV[22]) are derived from the imidazolium cations.

A sketch of cation chemistry in imidazolium ILs (Scheme 1) was given in the Introduction; using the results of section 3, it can be elaborated further.

First, our results indicate that the *deprotonation reaction (eq 4) occurs in all aromatic ILs.* This reaction is most facile for cations with long aliphatic arms, but the deprotonation also occurs (albeit to a small extent) even from the methyl arms. The resulting $R^{\bullet}(C^+)$ radicals can recombine and disproportionate with other radiolytically generated radicals (including other $R^{\bullet}(C^+)$ radicals) or add to double bonds and C(2) carbons.


dx.doi.org/10.1021/jp200305b |J. Phys. Chem. B 2011, 115, 3889–3902

Our results at very high cumulative doses suggest the occurrence of radiation-induced polymerization[7,20] with the $m/z$ of the product corresponding to ~4.5 monomer mass units (section 3.1.5). For $C_4$mim TfO, the radiolytic yield of the water insoluble polymer was ~0.23 monomer units per 100 eV at a cumulative dose of 6.7 MGy. This polymerization increases solvent viscosity, while reaction 4 results in acidification.

Second, we found that reactions 13a and 14 that lead to elimination of the side arms do not involve methyl groups. Furthermore, no clear-cut evidence for elimination for *n*-alkyl arms in reaction 14 is found, although there are examples of such elimination for alkoxy- and α-substituted alkyl arms. EPR observations of *delayed* elimination of the side arms in the 1,3-di(*tert*-butyl)imidazolium directly implicate reaction 14, yielding *N*-alkylimidazole ($Q_3$). As the latter species serves as a complexant for d- and f-ions, such a reaction may have a detrimental effect on the specificity of radionuclide separations. The protonated form of *n*-alkylimidazole, $Q_3H^+$, can also be generated via reaction 13a involving excitation of the parent cation. As the oxidized *n*-alkylimidazole, $Q_3^{+\bullet}$, recombines forming N−N bound multimers[20] (Scheme 1S in the Supporting Information), the loss of the side arm provides a chemical pathway to polymerization.

Third, a conceptually simple picture has emerged for reactions initiated by electron trapping in 1-methyl-3-alkylimidazolium liquids. The electron attaches to the cation, yielding the corresponding 2-imidazolyl radical. Further chemical transformations depend on the type of the ionic liquid. In class I ionic liquids, which includes most of the common anions (such as halides, acetates, alkyl sulfates, and alkanesulfonates, dialkyl phosphates, etc.), this 2-imidazolyl radical does not form a C(2)−C(2) bond with the parent cation; instead, it is protonated. If the parent cation is substituted at C(2), this protonation does not occur. In class II ionic liquids, the 2-imidazolyl radical reacts with the parent cation, forming a dimer radical cation (reaction 6) that also cannot be protonated. In both of these cases, electron trapping reaction 3 results in the formation of secondary *radical cations*, that is $Q_2H_2^{+\bullet}$ or $(Q_2H)_2^{+\bullet}$.

These observations contradict the common expectation that "ionization of ions" should lead to *neutral* radical chemistry. Coulomb interactions with the constituent ions increase the stability of reactive intermediates, so protonation and dimerization are energetically favored. In some imidazolium compounds, the $Q_2H_2^{+\bullet}$ cations persist at 300−350 K, which is uncommon for organic radicals. Such radical cations cannot disproportionate and/or recombine without undergoing deprotonation, which accounts for their remarkable stability. This persistence may account for low radiation stability of the imidazolium cations, as the steady-state concentration of such radicals is sufficiently high to facilitate cross-reactions leading to polymerization.

## 5. CONCLUDING REMARKS

In parts 1[1] and 2 of the present study, radiolytically induced reactions of anions and cations in imidazolium ionic liquids have been systematically examined. In agreement with previous studies,[8,18,22] it is shown that radiation stability of such ILs is comparable to that of molecular aromatic liquids, while their radiation chemistry is very complex. This chemistry can be viewed as prompt generation of primary neutral species (reactions 1−4) followed by their fragmentation, protonation, deprotonation, structural rearrangements, and the subsequent (secondary) chemistry when the resulting radicals and molecular fragments recombine, disproportionate, and react with stable radiolytic products. As these secondary reactions are determined by the primary radicals, we focused on the initiation of the reaction cascade. The methodological benefit of this approach is that it is possible to separate the overall chemistry into distinctive anion and cation chemistries.

It follows that radiolytic reactions of these ions are initiated primarily by redox reactions involving the constituent ions. Both cations *and* anions undergo reduction *and* oxidation. For anions, reduction is observed for aromatic and particular fluorinated anions (as well as certain other anions, such as hydrogen sulfate); otherwise, the anions primarily undergo oxidation. For the majority of common anions, this oxidation leads to irreversible fragmentation: decarboxylation, desulfonation, etc. For aliphatic cations, there is no prompt reduction by electron attachment, but aromatic cations are easily reduced; both types of cations are oxidized. This oxidation is followed by deprotonation from long aliphatic arms of the cations. The subsequent reactions of $R^\bullet(C^+)$ radicals slowly build polymers in irradiated ILs. The reduced imidazolium cation (2-imidazolyl) either persists (if the cations are substituted at 2-position) or becomes protonated (if these cations are not 2-substituted); in some ILs, these radicals can also add to the parent cation, forming the C(2)−C(2) bound dimer radical cation. In addition to these reactions, for some cations one observes elimination of their entire side arms. The latter reaction is most facile for α-substituted aliphatic and alkoxy arms, and the corresponding ILs should have reduced radiation stability as compared to *n*-alkyl derivatives.

As shown in part 1 of this study,[1] in some ILs (such as nitrates and trifluoroacetate) the radicals derived from imidazolium cations do not form, as most of the electrons and holes are trapped by the anion. Such a situation, however, is uncommon; in most of the ILs, both constituent ions are ionized. In the ILs composed of small, inorganic ions involving Cl and F, such as $Cl^-$, $BF_4^-$, and $PF_6^-$, halogen atoms are released that abstract H from the aliphatic arms of the cation via reaction 8, increasing the yield of $R^\bullet(C^+)$ radicals. Almost all of the anions typically used for IL synthesis fragment appreciably; we found only a few exceptions, such as benzoate and phthalimide anions. The resulting fragments are small, reactive radicals that add to the C(2) atom of the imidazolium ring and abstract H from the constituent ions. The dissociation of the constituent anions and deprotonation of the constituent cations result in generation of acid and volatilization. Cross recombination of different types of radicals results in polymerization of the constituent cations, which becomes rather substantial in the very high dose range, resulting in higher viscosity. The polymer product contains a significant fraction of decomposed imidazolium cations. Other detrimental effects of radiation involve the increased water solubility for hydrophobic ILs and the formation of imidazole and/or the protonated (imidazolium) cation via the loss of the side arms in the parent cation. As imidazole binds metal ions, such reactions may reduce extraction specificity. Similarly vexing is dealkylation in dialkylphosphate ILs, which results in the formation of monophosphates. However, since dialkylphosphates are already complexants, they would only be employed in extraction schemes where this characteristic was advantageous in the first place.

While radiation damage to the anionic component of the IL can be reduced by judicious choice or modification of the anion, little can be done to reduce the damage to simple imidazolium cations

by their structural variation. Unsubstituted imidazolium cations appear to be at a particular disadvantage in the view that the C(2) position can be readily attacked. This vulnerability is not present in 2-methylimidazolium and *N*-alkylpyridinium cations. The aliphatic chains are found to be another common locus of radiation damage. H loss due to deprotonation is compounded by H abstraction by anion-derived radicals. Using antioxidant anions, such as salicylates, suppresses extensive damage to the cations[1] for the price of more extensive damage to the anions. It is yet to be seen what compromise can result in the best long-term performance under radiation. One of the messages of our study is that attaching a ligand to a structural ion to produce a task-specific IL[26] would require a solid understanding of the radiolytic properties of the attached ion, as this ligand potentially would be covalently linked to a locus of radiation damage resulting in radical (ion) reactions involving the ligand.

While our examination was limited to neat ILs, extraction solvents based on such liquids typically contain extracting agents (e.g., ionophores) and these solvents are in contact with aqueous solutions that contain inorganic salts, bases, and acids (for example, nitric acid). As discussed in part 1[1] and section 3.1.4, addition of water to the IL had considerable effect on its chemistry as the hydronium ion yields highly reactive $H^{\bullet}$ atoms. Furthermore, nitrate serves as an efficient electron and hole scavenger that competes with imidazolium ions. Therefore, the mechanistic insight obtained in radiolysis studies of neat ILs is only one part of the considerations involving extraction solvents operating under realistic conditions.

It may also be questioned whether studies of radiation stability of such extraction solvents should be focused on the degradation of the *solvent* as opposed to that of the extracting agents. In our previous publication,[4] we demonstrated that addition of 20−40 wt % trimethylphosphate resulted in negligible production of methyl radicals. Elsewhere,[27] we examine the radiolytic degradation of crown ethers in ILs; in this case, too, the damage to the solvent is of a greater magnitude than the damage to the solute. Generalizing from these two examples, the radiation stability of extraction systems appears to be defined primarily by the radiation stability of the IL matrix. The situation is, typically, opposite in extraction systems based on molecular liquids (such as *n*-alkanes) where the extractants are the most radiation-sensitive components.

## ■ ASSOCIATED CONTENT

**Supporting Information.** (1) Section 1S with the synthetic methods, (2) Schemes 1S and 2S (reactions), (2) Tables 1S−5S (isotropic composition and hfcc's), and (2) Figures 1S−21S (EPR, $ESMS_1^+$, $^1H$ NMR spectra) with captions. This material is available free of charge via the Internet at http://pubs.acs.org.

## ■ AUTHOR INFORMATION

### Corresponding Author

*E-mail: shkrob@anl.gov. Tel: (630) 252-9516.

## ■ ACKNOWLEDGMENT

We thank D. M. Bartels, R. A. Crowell, S. Dai, M. L. Dietz, E. W. Castner, Jr., and K. Takahashi for stimulating discussions, R. Lowers, J. V. Muntean, S. Naik, and A. R. Tisch for technical assistance, Dr. W. Pitner (Merck KGaA, Darmstadt) for donation of the octylpyridinium tetracyanoborate, and Dr. Marie Thomas for the sample of $C_6$mim Br. The work at Argonne and Brookhaven was supported by the US-DOE Office of Science, Division of Chemical Sciences, Geosciences and Biosciences under contracts Nos. DE-AC02-06CH11357 and DE-AC02-98CH10886, respectively. Programmatic support via a DOE SISGR grant "An Integrated Basic Research Program for Advanced Nuclear Energy Separations Systems Based on Ionic Liquids" is gratefully acknowledged.

## ■ REFERENCES

(1) Shkrob, I. A.; Marin, T. W.; Chemerisov, S. D.; Wishart, J. F. *J. Phys. Chem. B* **2011**10.1021/jp2003062.

(2) Angel, R.; Worden, S. P.; Borra, E. F.; Eisenstein, D. J.; Foing, B.; Hickson, P.; Josset, J. L.; Ma, K. B.; Seddiki, O.; Sivanandam, S.; et al. *Astrophys. J.* **2008**, *680*, 1582–1594.

(3) Borra, E. F.; Seddiki, O.; Angel, R.; Eisenstein, D.; Hickson, P.; Seddon, K. R.; Worden, S. P. *Nature* **2007**, *447*, 979–981.

(4) Shkrob, I. A.; Chemerisov, S. D.; Wishart, J. F. *J. Phys. Chem. B* **2007**, *111*, 11786–11793.

(5) Shkrob, I. A.; Wishart, J. F. *J. Phys. Chem. B* **2009**, *113*, 5582–5592.

(6) Wishart, J. F.; Shkrob, I. A. In *Ionic Liquids: From Knowledge to Application*; Rogers, R. D.; Plechkova, N. V.; Seddon, K. R., Eds.; American Chemical Society: Washington, DC, 2009; pp 119−134. Wishart, J. F. *J. Phys. Chem. Lett.* **2010**, *1*, 3225–3231.

(7) Shkrob, I. A. *J. Phys. Chem. B* **2010**, *114*, 368–375.

(8) Keppler, A.; Himmerlich, M.; Ikari, T.; Marschewski, M.; Pachomow, E.; Hofft, O.; Maus-Friedrichs, W.; Endres, F.; Krischok, S. *Phys. Chem. Chem. Phys.* **2011**, *13*, 1174–1181.

(9) Wishart, J. F.; Neta, P. *J. Phys. Chem. B* **2003**, *107*, 7261–7267.

(10) (a) Wishart, J. F.; Lall-Ramnarine, S. I.; Raju, R.; Scumpia, A.; Bellevue, S.; Ragbir, R.; Engel, R. *Radiat. Phys. Chem.* **2005**, *72*, 99–104. (b) Katoh, R.; Yoshida, Y.; Katsumura, Y.; Takahashi, K. *J. Phys. Chem. B* **2007**, *111*, 4770–4774. (c) Asano, A.; Yang, J.; Kondoh, T.; Norizawa, K.; Nagaishi, R.; Takahashi, K.; Yoshida, Y. *Radiat. Phys. Chem.* **2008**, *77*, 1244–1247. (d) Kondoh, T.; Asano, A.; Yang, J. F.; Norizawa, K.; Takahashi, K.; Taguchi, M.; Nagaishi, R.; Katoh, R.; Yoshida, Y. *Radiat. Phys. Chem.* **2009**, *78*, 1157–1160.

(11) Behar, D.; Gonzalez, C.; Neta, P. *J. Phys. Chem. A* **2001**, *105*, 7607–7614.

(12) Marcinek, A.; Zielonka, J.; Gebicki, J.; Gordon, C. M.; Dunkin, I. R. *J. Phys. Chem. A* **2001**, *105*, 9305–9309.

(13) McKenzie, I.; Brodovitch, J.-C.; Percival, P. W.; Ramnial, T.; Clyburne, J. A. C. *J. Am. Chem. Soc.* **2003**, *125*, 11565–11570.

(14) Chandrasekhar, N.; Unterreiner, A.-N. *Phys. Chem. Chem. Phys.* **2010**, *12*, 1698–1708.

(15) Kuhl, O. *Chem. Soc. Rev.* **2007**, *36*, 592–607. Holloczki, H.; Gerhard, D.; Massone, K.; Szarvas, L.; Nemeth, B.; Veszpremi, T.; Nyulaszi, L. *New J. Chem.* **2010**, *34*, 3004–3009.

(16) Berthon, L.; Nikitenko, S. I.; Bisel, I.; Berthon, C.; Faucon, M.; Saucerotte, B.; Zorz, N.; Moisy, P. *Dalton Trans.* **2006**, 2526–2534.

(17) Bosse, E.; Berthon, L.; Zorz, N.; Monget, J.; Berthon, C.; Bisel, I.; Legand, S.; Moisy, P. *Dalton Trans.* **2008**, 924–931.

(18) Le Rouzo, G.; Lamouroux, C.; Dauvois, V.; Dannoux, A.; Legand, S.; Durand, D.; Moisy, P.; Moutiers, G. *Dalton Trans.* **2009**, 6175–6184.

(19) Lesimpe, A.; Mamer, O.; Miao, W.; Chan, T. H. *J. Am. Soc. Mass Spectrom.* **2006**, *17*, 85–95.

(20) Wang, H.-L.; O'Malley, R. M.; Fernandez, J. E. *Macromolecules* **1994**, *27*, 893–910.

(21) Allen, D.; Baston, G.; Bradley, A. E.; Gorman, T.; Haile, A.; Hamblett, I.; Hatter, J. E.; Healey, M. J. F.; Hodgson, B.; Lewin, R.; Lovell, K. V.; Newton, B.; Pitner, W. R.; Rooney, D. W.; Sanders, D.; Seddon, K. R.; Sims, H. E.; Thied, R. C. *Green Chem.* **2002**, *4*, 152–158.

(22) Tarabek, P.; Liu, S. Y.; Haygarth, K.; Bartels, D. M. *Radiat. Phys. Chem.* **2009**, *78*, 168–172.
(23) Hunt, P. A. *J. Phys. Chem. B* **2007**, *111*, 4844–4853.
(24) Berthon, L.; Chabronnel, M.-C. In *Ion Exchange and Solvent Extraction, A Series of Advances*; Moyer, B. A., Ed.; CRC Press: Roca Baton, FL, 2010; Vol. 19, pp 429−513.
(25) Ha, S. H.; Menchavez, R. N.; Koo, Y.-M. *Korean J. Chem. Eng.* **2010**, *27*, 1360–1365.
(26) Visser, A. E.; Swatloski, R. P.; Reichert, W. M.; Mayton, R.; Sheff, S.; Wierzbicki, A.; Davis, J. H.; Rogers, R. D. *Chem. Commun.* **2001**, 135–136.
(27) Shkrob, I. A.; Marin, T. W.; Dietz, M. L. *J. Phys. Chem. B*, published online March 16, http://dx.doi.org/10.1021/jp200307h.